HHS Public Access

Author manuscript

Mol Microbiol. Author manuscript; available in PMC 2016 August 12.

Published in final edited form as:

Mol Microbiol. 2015 December ; 98(6): 1037–1050. doi:10.1111/mmi.13172.

A thiol-disulfide oxidoreductase of the Gram-positive pathogen *Corynebacterium diphtheriae* is essential for viability, pilus assembly, toxin production and virulence

Melissa E. Reardon-Robinson[1], **Jerzy Osipiuk**[2,3], **Neda Jooya**[1], **Chungyu Chang**[1], **Andrzej Joachimiak**[2,3], **Asis Das**[4], and **Hung Ton-That**[1,*]

[1]Department of Microbiology & Molecular Genetics, University of Texas Health Science Center, Houston, TX, USA

[2]Midwest Center for Structural Genomics, Department of Biosciences, Argonne National Laboratory, Argonne, IL, USA

[3]Structural Biology Center, Department of Biosciences, Argonne National Laboratory, Argonne, IL, USA

[4]Department of Molecular Biology and Biophysics, University of Connecticut Health Center, Farmington, CT, USA

Summary

The Gram-positive pathogen *Corynebacterium diphtheriae* exports through the Sec apparatus many extracellular proteins that include the key virulence factors diphtheria toxin and the adhesive pili. How these proteins attain their native conformations after translocation as unfolded precursors remains elusive. The fact that the majority of these exported proteins contain multiple cysteine residues and that several membrane-bound oxidoreductases are encoded in the corynebacterial genome suggests the existence of an oxidative protein-folding pathway in this organism. Here we show that the shaft pilin SpaA harbors a disulfide bond in vivo and alanine substitution of these cysteines abrogates SpaA polymerization and leads to the secretion of degraded SpaA peptides. We then identified a thiol-disulfide oxidoreductase (MdbA), whose structure exhibits a conserved thioredoxin-like domain with a CPHC active site. Remarkably, deletion of *mdbA* results in a severe temperature-sensitive cell division phenotype. This mutant also fails to assemble pilus structures and is greatly defective in toxin production. Consistent with these defects, the Δ*mdbA* mutant is attenuated in a guinea pig model of diphtheritic toxemia. Given its diverse cellular functions in cell division, pilus assembly and toxin production, we propose that MdbA is a component of the general oxidative folding machine in *C. diphtheriae*.

[*]For correspondence. ton-that.hung@uth.tmc.edu; Tel. (+1) 713 500 5468; Fax (+1) 713 500 5499.

Supporting information

Additional supporting information may be found in the online version of this article at the publisher's web-site.

Introduction

Corynebacterium diphtheriae is a Gram-positive actinobacterium that is infamous for its secretion of a highly potent toxin that causes diphtheria, a deadly disease for unvaccinated individuals (Rogers *et al.*, 2011). Diphtheria toxin (DT) is a canonical A-B toxin comprised of a catalytic domain A, and transfer-mediating domain B. Following cleavage of the N-terminus by a host-derived endopeptididase, the domains remain linked by a single disulfide bond, which permits the release of domain A upon its entry into the reducing host cytoplasm (Collier, 2001). In addition, domain B contains another disulfide bond, which presumably aids in protein folding and stability (London, 1992). *C. diphtheriae* pathogenesis is also dependent on three types of adhesive pili that are assembled by a sortase-mediated mechanism (Ton-That and Schneewind, 2003; Mandlik *et al.*, 2007). Similar to DT, all corynebacterial pilins possess a signal peptide sequence, apparently required for SecA-mediated translocation of unfolded protein precursors. A model of pilin export and assembly has been proposed for the archetype SpaA pili. According to this model (Mandlik *et al.*, 2008; Reardon and Ton-That, 2013), pilin precursors are transported out of the cell by the Sec apparatus in an unfolded states, and then are retained within the extracytoplasmic face of the membrane by a C-terminal cell wall sorting signal (CWSS). This CWSS is required for sortase-catalyzed polymerization that joins individual subunits into a pilus polymer. The resulting polymers are ultimately linked to the bacterial cell wall via lipid II precursor. How pilins and DT are folded after translocation remains a fundamental question.

In Gram-negative bacteria, disulfide bond formation is critical for posttranslocational folding of proteins secreted into the oxidizing environment of the bacterial periplasm. In *Escherichia coli*, DsbA – the archetype of Gram-negative thiol-disulfide oxidoreductases (Bardwell *et al.*, 1991) – oxidizes free thiol groups in nascent proteins emerging from the Sec translocon by donating a reactive disulfide bond within a catalytic CxxC motif (Kadokura and Beckwith, 2009). In turn, the DsbA active site is reduced and requires reoxidation by DsbB, a membrane-bound oxidoreductase (Bardwell *et al.*, 1993; Missiakas *et al.*, 1993). Recycling activities of the redox pair DsbA/DsbB is dependent on quinone, a component of the electron transport chain (Kobayashi and Ito, 1999). Importantly, because many Gram-negative virulence factors, such as flagella, adhesive pili and toxins, require disulfide bond formation, disulfide bond-forming machinery is key for virulence in a number of Gram-negative pathogens, including *E. coli*, *Shigella flexneri*, *Pseudomonas aeruginosa*, *Bordetella pertussis, Neisseria meningitidis* and *Salmonella enterica* (Heras *et al.*, 2009).

By comparison, oxidative protein folding within Gram-positive bacteria has not been fully explored. The Gram-positive cell envelope is comprised of a single cytoplasmic membrane, hence called monoderm (Gupta, 1998), and so is considered devoid of a periplasmic space. Curiously, DsbA-like proteins have been identified in several Gram-positive organisms, but most are encoded in operons with specific substrates, unlike that in Gram-negative bacteria (Dorenbos *et al.*, 2002; Meima *et al.*, 2002; van der Kooi-Pol *et al.*, 2012). In *Bacillus subtilis, dsb*-like genes are located within a competence gene cluster, and required for formation of the Com GC pilus (Meima *et al.*, 2002). Only DsbA was found in *Staphylococcus aureus* (Dumoulin *et al.*, 2005), and its function has also recently been implicated in stability of the ComGC pseudopilin (van der Kooi-Pol *et al.*, 2012). More

recently, a paralogous thiol-disulfide oxidoreductase in *Streptococcus gordonii* called SdbA has been linked to disulfide bond formation of autolysin AtlS (Davey *et al.*, 2013). Unlike Firmicutes, Actinobacteria, including *Corynebacterium*, *Streptomyces* and *Mycobacterium*, secrete a large number of polypeptides with multiple Cys residues and encode thiol-oxidoreductase proteins (Daniels *et al.*, 2010). Intriguingly, expression of a *Mycobacterium tuberculosis* oxidoreductase, annotated as Vitamin K epoxide reductase (VKOR), was able to rescue the defects of the *E. coli dsbB* mutant (Dutton *et al.*, 2008). A DsbA-like protein has been reported in this organism (Chim *et al.*, 2013; Premkumar *et al.*, 2013). More recently, a disulfide bond forming machine has been identified in *Actinomyces oris* (Reardon-Robinson *et al.*, 2015). These findings support the notion that Actinobacteria may utilize general oxidative protein folding in their exoplasm.

Here we describe a disulfide bond-forming machine for Sec-transported proteins in the actinobacterium *C. diphtheriae*. We demonstrate that the SpaA pilin of *C. diphtheriae* contains a disulfide bond that is essential for pilus assembly. Genetic and biochemical studies revealed that disulfide bond formation is catalyzed by a membrane-tethered thiol-disulfide oxidoreductase enzyme termed MdbA (mdb for monoderm disulfide bond-forming). Structure determination by X-ray crystallography showed the presence of a thioredoxin-like domain, typical of thiol-disulfide oxidoreductases. Importantly, we showed that the chaperone functions of MdbA are not limited to the pilins, as MdbA is essential for proper folding and stability of the diphtheria toxin. Furthermore, the *mdbA* mutant is defective in cell division at 37°C and also attenuated in virulence. Therefore, we propose that MdbA is a major disulfide bond-forming machine in *C. diphtheriae* that may serve as an important target for the development of antimicrobial therapies.

Results

Disulfide bond formation is required for pilus assembly in *C. diphtheriae*

Crystallization studies of the pilus shaft SpaA protein predicted that the C-terminal IgG-like domain contains a disulfide bond formed between cysteine (Cys) residues C383 and C443 (Kang *et al.*, 2009) (see Fig. 1A). To probe the presence of this bond in vivo, we used methoxypolyethylene glycol-maleimide (Mal-PEG), a 2-KDa alkylating agent that forms stable thioether bonds with free sulfhydryl groups (Makmura *et al.*, 2001), which can be detected by a change of protein mobility using SDS-PAGE. SpaA monomers were collected from the culture medium of a *C. diphtheriae* mutant (HT3) that secretes SpaA monomers (Swaminathan *et al.*, 2007), trichloroacetic acid (TCA) precipitated and then acetone washed. The resulting samples were resuspended in buffer with or without DTT, and subsequently incubated with Mal-PEG. After removal of Mal-PEG by TCA precipitation, SpaA was detected by Western blotting using SpaA specific antibodies (α-SpaA). In the absence of DTT, Mal-PEG treatment did not alter migration of SpaA monomers (Fig. 1B; lanes 1 and 3). In contrast, reduction of SpaA with DTT prior to Mal-PEG treatment resulted in an upshift of the SpaA band (Fig. 1B; last lane), indicating that the pilin contains a disulfide bond in vivo.

We next examined whether the formation of this C-terminal disulfide bond is required for pilus assembly. A plasmid expressing SpaA harboring alanine-substitutions of C383 or C443

was introduced into a *spaA* deletion mutant (Δ*spaA*). Corynebacterial cells were subject to cell fractionation and protein samples were analyzed by Western blotting with (α-SpaA) (see Methods). Compared with cells expressing wild-type SpaA (Fig. 1C; lanes WT and pSpaA), no pilus polymers (marked P) were detected in the cell wall (W) fractions of the Cys-to-Ala mutants; instead, low-molecular-weight species of SpaA were detected in the culture medium (S) fractions (Fig. 1C; last four lanes). Cell surface assembly of pili was also examined by immunogold electron microscopy (IEM). Corynebacteria were immobilized on carbon-coated nickel grids, blotted with α-SpaA, followed by IgG antibodies conjugated to gold particles. Consistently, no pili were observed on the surface of C383A or C443A mutants (Fig. 1D). Together, these results demonstrate that the SpaA C383-C443 linkage is essential for pilus assembly.

Identification of a thiol-disulfide oxidoreductase in *C. diphtheriae* by X-ray crystallization

The *C. diphtheriae* genome encodes several putative membrane-bound oxidoreductases, including DIP0397, DIP1880 and DIP0411, that may participate in oxidative protein folding. DIP0411 is a proposed DsbF homolog and its crystal structure reveals a thioredoxin-like domain with a conserved catalytic CxxC motif (Um *et al.*, 2014). However, its localization with genes encoding c-type cytochrome synthesis components suggests it may be involved with energy production rather than protein folding (Kanehisa and Goto, 2000). DIP0397 is predicted to encode a 32-kDa membrane-bound protein with a CPFC motif. A deletion of the gene encoding DIP0397 produced no detectable phenotypes, so it was not studied further (data not shown). Finally, DIP1880, which we renamed MdbA (*mdb* for monoderm disulfide bond-forming), is predicted to encode a 27-kDa transmembrane protein that harbors a CPHC motif. Cell fractionation and immunoblotting with antibodies against MdbA (α-MdbA) revealed that the protein is membrane localized (see Fig. 3A). We have recently shown that DIP1880 has thiol-oxidoreductase activities in vitro (Reardon-Robinson *et al.*, 2015).

To reveal the structural identity of MdbA, we purified the recombinant protein from *E. coli* for X-ray crystallization using seleno-methionine single-wavelength anomalous diffraction (SAD). The reduced form of MdbAwas refined to 1.77-Å resolution with R-work and R-free factors equal to 16.9% and 21.0% respectively (Tables 1 and 2). The structure harbors a thioredoxin-like domain and an extended α-helical domain (Fig. 2A), typical of the DsbA protein family (Martin *et al.*, 1993; Shouldice *et al.*, 2011). The thioredoxin-like domain is composed of a 6-strand β-sheet in an order of β0↓- β1↑- β3↓- β2↓- β4↑- β5↓ and 2 flanking α helices, H1 and H7, based on a previous secondary structure numbering system (Martin *et al.*, 1993). The β-sheet also includes an additional β0 strand at the N-terminus, presumably as a result of different positioning and/or higher completeness of the MdbA N-terminus, as compared with other Gram-positive DsbA-like structures (Fig. S1). The α-helical domain consists of 6 α-helices (H2–H6 and H3*) and two 3_{10} helices (Fig. 2A and S1). Unlike other DsbA-like proteins, the *C. diphtheriae* MdbA structure contains a unique secondary structure element, which is the short α-helix H3* (residues 163–166) right after helix H3. The CPHC active-site motif (residues 91–94) resides on the N-terminal end of helix H1 (Fig. 2B). Significantly, the MdbA structure also harbors a conserved *cis*-Pro loop (residues S221 and P222) characteristically found in the TRX-related proteins (Ren *et al.*, 2009). Situated on the

loop between H6 α-helix and β5 strand, the *cis*-Pro element interacts with the CPHC motif via a hydrogen bond formed between S221 and C91 (3.07 Å distance, Fig. 2B).

Based on DALI server analysis (Holm and Rosenstrom, 2010), the MdbA structure is closely related to the crystal structure of Rv2969c, a DsbA-like protein from *M. tuberculosis* (PDB: 4K6X) (Premkumar *et al.*, 2013) (Fig. 2C), with Z-score and RMSD of 19.2 and 2.3, respectively, for 199 residues. Other similar structures include from *B. subtilis* BdbD (PDB: 3EU3) (Crow *et al.*, 2009) and *S. aureus* DsbA (PDB: 3BCI) (Heras *et al.*, 2008) (Fig. 2D and E). On the other hand, the *E. coli* DsbA structure (PDB:1A2L) (Martin *et al.*, 1993) (Fig. 2F) is farther down on the DALI homolog list with Z-score and RMSD values equal to 11.4 and 3.7 respectively. Notably, the β-sheet topology of the *C. diphtheriae* MdbA structure is different from the *E. coli* DsbA and most of DsbA-family proteins of Gram-negative bacteria – the β-strand order of 0-1-3-2-4-5 compared with 3-2-4-5-1 in *E. coli*. Altogether, the results support that the *C. diphtheriae* MdbA is a thiol-disulfide oxidoreductase.

Essential roles of *C. diphtheriae* MdbA in cell division, pilus assembly, toxin production and disulfide bond formation

To examine the role of *C. diphtheriae* MdbA in vivo, we generated a nonpolar deletion mutant of *mdbA*. Strikingly, excision of this gene resulted in a severe growth defect at 37°C, while growth at 30°C was similar to that of the wild-type strain (Fig. 3B). When examined by electron microscopy, the Δ*mdbA* mutant was indistinguishable from wild-type at 30°C. However, when shifted to 37°C, Δ*mdbA* became chained, clumped and coccoid in appearance (Fig. 3C–E). To examine cell growth, we labeled corynebacteria with fluorescent vancomycin to visualize nascent peptidoglycan insertion by fluorescence microscopy. Fluorescence signal was detected at the septum and cell poles of the wild-type strain, consistent with apical growth of *C. diphtheriae* (Umeda and Amako, 1983); however, fluorescence signal was defused throughout the cell envelope of the Δ*mdbA* mutant (Fig. 3F and G). To probe a potential defect in cell wall synthesis, we tested *C. diphtheriae* susceptibility to β-lactams ampicillin and penicillin. Remarkably, Δ*mdbA* growth was inhibited at lower concentrations of antibiotics than WT (Fig. 3H). Altogether, the data suggest that *mdbA* is required for proper growth and division.

As pilus assembly is coupled with cell growth, pilus polymerization within the Δ*mdbA* mutant was examined by Western blotting using culture medium and cell wall fractions of bacteria grown at 30°C. Compared with wild-type corynebacteria, the Δ*mdbA* mutant did not produce any SpaA polymers, but complementation of this mutant with plasmid-borne copies of *mdbA* rescued this defect (Fig. 4A). Significantly, complementation was dependent on an intact CxxC active as alanine-substitution of MdbA C94 abrogated pilus assembly (see Fig. 5B).

By bioinformatics analysis (Kanehisa and Goto, 2000), we found that more than 60% of proteins secreted by *C. diphtheriae* contain two or more cysteine residues. Therefore, we hypothesized that MdbA targets an array of substrates. To investigate this, we chose diphtheria toxin (DT) as a nonpilus protein model. DT is a protein synthesis inhibitor that belongs to the A-B family of toxins. Secreted by *C. diphtheriae* when bacteria encounter low

iron, DT contains two disulfide bonds; the first disulfide bond loops the active domain A and the binding domain B, and is essential for toxin function (Boquet and Pappenheimer, 1976) (Fig. 4B). DT production was induced by adding a metal chelator to *C. diphtheriae* cultures, isolated by centrifugation, and then TCA precipitated. DT was then detected by Western blotting using monoclonal antibodies against the A fragment of the toxin (α-DT). DT from the wild-type strain was detected as a single band running at approximately 60 kDa as predicted (Fig. 4C). Deletion of *mdbA*, however, resulted in the production of multiple bands; the intensity of the band seen in wild-type cells is reduced with the concomitant accumulation of a low-molecular weight product(s) (Fig. 4C). In the absence of *mdbA*, this result suggested that DT is prone to degradation. Complementation of this mutant by wild-type *mdbA* rescued normal production of this toxin (Fig. 4C).

To test if the observed phenotype was caused by the failure to form disulfide bonds, we again turned to alkylation. Harvested DT was suspended in buffer with or without DTT, treated with Mal-PEG, and detected by Western blotting. DT obtained from wild-type cells showed no change in protein migration unless the sample was first treated with reducing DTT (Fig. 4D; first four lanes), indicating that secreted DT is oxidized. However, DT released by the Δ*mdbA* mutant was readily modified by Mal-PEG, demonstrating that it was released with reduced Cys residues (Fig. 4D, last two lanes). Note that the level of secreted DT in the Δ*mdbA* mutant was significantly reduced, consistent with the observation in Fig. 4C that DT is more susceptible to degradation when *mdbA* is absent.

The failure of the Δ*mdbA* mutant to form disulfide bonds in DT was also shown by examining the N-terminal disulfide bond that connects theAand B domains (Fig. 4E). Harvested DT was treated with furin, a protein that cleaves an Arg-XX-Arg motif between the A and B domains. Upon cleavage, the A and B domains are linked by a single disulfide linkage in the N-terminus. Following furin treatment, the samples were incubated with the reducing agent β-mercaptoethanol (BME) to separate the domains. In the sample obtained from wild-type cells, release of the A domain was detected only after BME treatment with BME. However, the release of the A domain in the sample obtained from Δ*mdbA* was detected immediately after furin cleavage, indicating that the disulfide bond between the domains was not formed. Expression of MdbA in the Δ*mdbA* mutant restored the wild-type pattern (Fig. 4E). Collectively, these results support the view that MdbA is required for disulfide bond formation within pilus and nonpilus virulence factors in *C. diphtheriae*.

Conservation of oxidative protein folding machinery

As MdbA is more closely related to *M. tuberculosis* (*Mtb*) DsbA, it is logical to determine if expression of *Mtb* DsbA would rescue the defects of the *C. diphtheriae* Δ*mdbA* mutant. However, the effort failed after several attempts to clone the *Mtb dsbA* gene in *C. diphtheriae*, possibly due to codon specificity. We then cloned the *E. coli* DsbA containing the transmembrane domain of MdbA into the *C. diphtheriae* Δ*mdbA* mutant (Fig. 5A; $DsbA_{TM}$). Pilus assembly was assessed by Western blotting as described in Fig. 4A with protein samples collected from the recombinant DsbA strain grown at 30°C. Remarkably, the Δ*mdbA* mutant expressing the membrane-tethered *E. coli* DsbA produced SpaA pilus polymers at the levels similar to that of the wild-type and MdbA complementing strains

(Fig. 5B). However, this strain still exhibited slight cell morphology defects at 37°C (Fig. 5C–E), suggesting that the *E. coli* DsbA enzyme might not be fully functional.

Requirement of the disulfide bond-forming machine MdbA for *C. diphtheriae* virulence

As *C. diphtheriae* MdbA is required for the assembly of SpaA-type pili, as well as the production DT, we hypothesized that MdbA is an important virulence factor. To test this, we employed a guinea pig model of diphtheritic toxemia (Young and Mood, 1945; Pappenheimer *et al.*, 1957). In this experiment, groups of six animals were injected via the intraperitoneal route (IP) with 2.5×10^7 CFU of the wild-type, Δ*tox*, Δ*spaA-I* or Δ*mdbA* strain, and animal survival was monitored over 7 days (Fig. 6). Within 2 days, 80% of guinea pigs inoculated with wild-type corynebacteria succumbed to infection. The Δ*tox* mutant, which does not produce diphtheria toxin, did not cause a lethal infection as expected. Remarkably, strains devoid of MdbA or all pili were significantly attenuated as well. There was little or no significant difference between the Δ*tox* mutant strain and the Δ*mdbA* mutant or the Δ*spaA-I* mutant. These data demonstrate that MdbA is an important virulence factor for *C. diphtheriae*.

Discussion

It is well known that oxidative protein folding in Gram-negative bacteria occurs in the oxidizing environment of their periplasmic space. Due to the lack of an outer membrane, however, the Gram-positive bacteria are generally not considered to possess an oxidative periplasm. Therefore, whether an oxidative protein-folding pathway exists in monoderm bacteria is an outstanding question. We report here our systematic investigation of a disulfide bond-forming enzyme MdbA that may serve as a general oxidative folding machine to fold exported proteins in *C. diphtheriae*.

To search for an oxidative folding machine in this organism, we employed two model exported proteins – SpaA and the diphtheria toxin, which are respectively predicted to and known to contain disulfide bonds. SpaA, the major subunit of the SpaA-type pili, is predicted to harbor a single disulfide bond between the residues C383 and C443 in the C-terminus. We confirmed the formation of this linkage in vivo using an alkylation assay (Fig. 1). Importantly, Cys-to-Ala mutations abolished pilus assembly, indicating that this linkage is essential for SpaA structure-function. We subsequently went on to identify the *C. diphtheriae* MdbA as a potential disulfide bond-forming enzyme through bioinformatics analysis. To determine if MdbA is indeed a thiol-oxidoreductase, we solved the 3-D structure of MdbA by X-ray crystallography. Like numerous thiol-oxidoreductases, *C. diphtheriae* MdbA has a signature thioredoxin-like domain and an extended α-helix (Fig. 2). Importantly, MdbA Cys residues are found within the CXXC catalytic site that interacts with a conserved *cis*-Pro loop. Comparisons of *C. diphtheriae* MdbA structure with other thiol-oxidoreductases revealed that it is more related to the mycobacterial DsbA than a structure solved for the well-known disulfide bond forming protein in *E. coli*.

Importantly, unlike Dsb proteins of *E. coli*, *C. diphtheriae* MdbA is a membrane-tethered enzyme (Fig. 3). We suspect that this may be an adaptation to the absence of an enclosed periplasmic compartment as *E. coli dsbA* rescued Δ*mdbA* phenotypes only if it was fused to

a membrane anchor (Fig. 5B; data not shown). Remarkably, although the *C. diphtheriae mdbA* deletion mutant divided normally at 30°C, the cells exhibited a severe growth defect at 37°C. Electron microscopy revealed that the normally rod-shaped bacteria displayed chained morphology, and a coccoid-like appearance when shifted to the nonpermissive temperature. It is noteworthy that a previous study found that the penicillin-binding proteins (PBPs) expressed by *Corynebacterium glutamicum* were important for proper cell growth and division (Valbuena *et al.*, 2007). Deletion of genes encoding these proteins caused similar morphological phenotypes observed with Δ*mdbA*. Not surprisingly, surveys of the *C. diphtheriae* genome revealed multiple PBPs with multiple Cys residues including PBP1a, PBP1b, PBP2a and PBP2b. PBP1b and PBP2b, which are synthetically lethal in *C. glutamicum* (Valbuena *et al.*, 2007), possess 9 and 4 Cys residues respectively. We suspect that, similar to SpaA and DT, PBPs require oxidative folding. These proteins likely fail to fold properly in the absence of *mdbA*, thereby becoming nonfunctional and/or susceptible to proteolysis. In support of this, *C. diphtheriae ΔmdbA* was much more susceptible to antibiotics that target PBP function (Fig. 3). We speculate that at lower temperatures, exogenous sources of oxidation may fold enough PBPs to maintain proper cell growth. However, at 37°C, residual PBPs may not be sufficient to meet the demands of rapid cellular replication, and as a consequence, these bacteria eventually stop dividing. The role of MdbA in bacterial division will be the focus of future studies.

Importantly, we were able to establish the essential function of oxidative protein folding using two different model substrates. Deletion of *mdbA* abrogates pilus assembly (Fig. 4), and this is consistent with a defect in pilus polymerization when the C-terminal SpaA disulfide bond is disrupted (Fig. 1). These data demonstrate that the thiol-oxidoreductase MdbA machine is a required component of the pilus assembly pathway. Interestingly, although the *C. diphtheriae* MdbA structure is less similar than the *E. coli* DsbA, ectopic expression of the *E. coli* DsbA with the MdbA transmembrane domain rescued the pilus assembly defect at 30°C temperature (Fig. 5), thus providing additional support for conservation of the oxidative folding reaction mechanisms between Gram-positive and Gram-negative organisms.

As a vast number of *C. diphtheriae* exported proteins (~ 60%) secreted through the Sec translocon harbor two or more Cys residues, we hypothesized that MdbA may function as a general protein folding factor. To validate this conjecture, we probed the well-known exotoxin DT that contains two bona fide disulfide bonds. Production of full-length DT was significantly reduced in the Δ*mdbA* mutant with significant accumulation of degradation products (Fig. 4). By a combination of alkylation and furin-cleavage assays, we demonstrated that the *mdbA* mutant secretes a reduced form of DT, irrefutable evidence that MdbA is required for disulfide bond formation in vivo.

Because MdbA is required for optimal cell growth as well as the production of two virulence factors that are important for colonization and cytotoxicity, MdbA must be a major virulence factor for successful infection by corynebacteria. We tested this logical hypothesis with an animal survival assay using the guinea pig model of diphtheritic toxemia, expecting that the Δ*mdbA* mutant, similar to Δ*tox*, would be nonvirulent. Indeed, while the majority of animals inoculated with wild-type *C. diphtheriae* succumbed to infection and died shortly, most of

the animals exposed to the Δ*mdbA* mutant survived (Fig. 6). Notably, some animals infected with the Δ*mdbA* mutant were killed. This result seems somewhat surprising as *C. diphtheriae* Δ*mdbA* displays a growth defect at 37°C, the host's normal body temperature. However, it is important to recall that DT production is normally triggered by unfavorable growth conditions, i.e. when cells are not dividing. An alkylation experiment did reveal that Δ*mdbA* secreted DT with reduced Cys residues, but a small portion of full-length toxin was not reactive (Fig. 5), suggesting that some of the toxin contained disulfide bonds. It is conceivable that spontaneous protein oxidation in the host environment permitted the proper folding of a sufficient amount of DT to cause the lethal infection in some, but not all of the animals. We propose that MdbA would serve as an ideal target to develop antimicrobials against Actinobacterial pathogens including *M. tuberculosis*. The fact that the Δ*mdbA* mutant is highly sensitive to β-lactams, a combination of MdbA inhibitors with additional antibiotics, may provide an effective antimicrobial strategy.

Finally, it is noteworthy to point out that the cell envelope of the genus *Corynebacterium* contains an outer layer of mycolic acids that may function as an outer membrane (Bayan *et al.*, 2003; Burkovski, 2013). Indeed, freeze fracture cryo-EM provides physical evidence for the presence of this outer 'mycomembrane' in *Mycobacterium bovis* BCG, *Mycobacterium smegmatis* and *C. glutamicum* (Zuber *et al.*, 2008). Thus, it is possible that *C. diphtheriae* possess an equivalent periplasmic compartment to regulate oxidative protein folding. We propose that as protein precursors emerge from the Sec translocon, they form a mixed-disulfide intermediate with MdbA (Fig. 7). Here, MdbA acts as a 'place-holder' (Kosuri *et al.*, 2012) until a second Cys residue within the substrate is positioned to resolve the mixed-disulfide bond, which results in the formation of the disulfide linkage and the completion of substrate folding. In turn, the MdbA CxxC motif is reduced to an inactive state. It is likely that another thiol-oxidoreductase, we termed MdbB, would reoxidize MdbA. Its identity and functionality will be subject of future investigation.

Experimental procedures

Bacterial strains, primers, plasmids and media

Bacterial strains, primers and plasmids used in this study are listed in Tables S1 and S2 of Supplemental Information. *Corynebacterium* strains were grown in Heart Infusion (HI) broth or HI agar plates. *E. coli* DH5α and BL21, used for molecular cloning and protein purification, respectively, were grown in Luria Broth (LB) or agar. Kanamycin (Kan) was added at 50 μg ml^{-1} when needed.

Construction of recombinant plasmids

pMdbA—Primers *mdbA*_BamHl_F and *mdbA*_BamHl_R were designed to PCR-amplify the promoter and coding regions of *C. diphtheriae mdbA* with appending BamHI sites. The DNA fragment was digested with the appropriate restriction enzyme, and cloned into pCGL0243 pretreated with alkaline phosphatase and BamHI. The resulting plasmid was electroporated into NJ2.

pDsbA$_{TM}$—The primers *dsbA*$_{Ec}$_F and *dsbA*$_{Ec}$_R_BamHI were used to PCR amplify the extracellular regions of *E. coli dsbA* using Phusion DNA polymerase® (NEB) to generate blunt ends. The resulting product was 5′ phosphorylated and cut with BamHI. Segments encoding the promoter, RBS, and cytoplasmic and transmembrane domains for *C. diphtheriae mdbA* were amplified with primers P*mdbA*_F_BamHI and P*mdbA*TM_R, and then digested with BamHI. Both DNA fragments then were ligated with pCGL0243 precut with BamHI and treated with alkaline phosphatase (NEB) to generate the recombinant plasmid, which was electroporated into NJ2.

Recombinant vectors using pMCSG7—To generate recombinant, His-tagged MdbA proteins, primers (see Tables S1 and S2) were designed to amplify the extracellular-coding regions of *C. diphtheriae mdbA*. The resulting PCR products were cloned into pMCSG7 using ligation-independent cloning (Stols *et al.*, 2002). Purified DNA fragments were treated with LIC-competent T4 DNA polymerase (Novagen) and 2.5 μM dCTP. Meanwhile, pMCSG7, precut with SspI, was treated with LIC-competent T4 polymerase and dGTP to generate complementary overhangs between the linearized vector and *mdbA*. The products were then incubated over a gradient of temperatures (3 min at 70°C, 2 min at 65°C, 2 min at 60°C, 2 min at 55°C, 1 min at 50°C, 1 min at 45°C, 1 min at 40°C, 1 min at 35°C, 1 min at 30°C, 5 min at 25°C) to promote annealing. The resulting plasmids were used to transform *E. coli* DH5α and the insert was confirmed by DNA sequencing. The plasmids were then introduced into *E. coli* BL21 (DE3) for protein expression.

Site-directed mutagenesis of recombinant plasmids

To generate cysteine-to-alanine mutations within SpaA, inverse PCR was utilized using recombinant plasmids as templates (Table S2). Appropriate primers (Table S1) carrying the desired mutations were 5′ phosphorylated and used to PCR-amplify the plasmid templates with Phusion HF DNA polymerase (NEB). The resulting linear products were purified products, treated with ligase to reform the circular plasmids, and used to transform *E. coli* DH5α. DNA sequencing confirmed the desired mutations, and the plasmids were introduced to the appropriate strains (Table S2).

Generating gene deletions in *C. diphtheriae*

Nonpolar, in-frame deletion mutants were generated using the SacB counter-selection protocol as reported by Ton-That and Schneewind (2003). Briefly, approximately 1 Kb-fragments up- and downstream of the genes of interest were cloned into the integration plasmid pK19mobsacB expressing Kan resistance and *sacB* genes (Schafer *et al.*, 1994). The resulting plasmid was introduced into *E. coli* S17-1 for conjugation with *C. diphtheriae*. Integration clones were selected for growth on Kan and nalidixic acid. To induce a double-crossover event leading to plasmid excision, *C. diphtheriae* were grown overnight without antibiotics. Loss of the integrated plasmid was selected for growth on HI agar plates containing 1% sucrose, which is toxic to cells expressing *sacB*. Gene deletions were identified by PCR and analyzed by Western blotting.

Cell fractionation and Western blotting

Overnight cultures of *C. diphtheriae* strains were used to inoculate fresh cultures (1:50 dilution). Cells grown at 30°C or 37°C to mid-log phase were normalized to an OD_{600} of 1.0, and subject to centrifugation to separate the medium (S) and cell fractions. *C. diphtheriae* were washed and re-suspended in hydrolase buffer [SMM, 0.5M sucrose, 10 mm $MgCl_2$, phosphate buffered saline (PBS) pH 7.4], and then incubated with cell wall hydrolase enzymes at 37°C for 3 h. After treatment, the soluble cell wall fractions (W) were separated from the protoplasts (P) by centrifugation. P fractions were then washed in SMM buffer, resuspended in PBS containing 0.1% Triton-114, and subjected to three freeze/thaw cycles using dry ice-ethanol and 100°C water baths. When needed, the cytoplasmic fraction (C) was isolated by ultracentrifugation of lysed protoplasts prior to TCA precipitation. The S, W and C fractions were TCA precipitated and acetone washed. Protein samples were resuspended in reducing or nonreducing SDS loading buffer, heated at 60°C for 10 minutes, and separated on Tris-glycine gels. Proteins were detected with rabbit-raised antisera diluted in 5% milk (1:20 000 for α-SpaA; 1:20 000, α-MdbA; or 1:1000, α-DT) followed by horseradish peroxidase (HRP) (1:10 000) conjugated goat anti-rabbit IgG for detection by chemiluminescence.

Protein purification and crystallography

The recombinant MdbA protein for crystallography expressed from pMCSG7-MdbA was purified from *E. coli* cells grown in M9 medium supplemented with ampicillin (100 μg ml^{-1}). A selenomethionine (SeMet) derivative of the expressed MdbA protein was prepared as previously described (Walsh *et al.*, 1999). Harvested cells were disrupted by sonication, and clear lysates were obtained by centrifugation. The recombinant protein was purified by affinity chromatography using Ni-NTA (Qiagen) in the presence of 5 mM β-mercaptoethanol. After digestion with 0.15 mg TEV protease (ratio of 1.5:200) for 16 h at 4°C, the cleaved proteins were passed through a Ni-NTA column for removal of the TEV enzyme and cleaved N-terminal tags. Subsequently, the protein was further purified by gel-filtration on a HiLoad 16/60 Superdex 200 pg column (GE Healthcare) in 10 mM HEPES buffer pH 7.5, 200 mM NaCl and 1 mM DTT. The protein was concentrated up to 40 mg ml^{-1} concentration using Amicon Ultracel 10K centrifugal filters (Millipore).

The initial crystallization condition was determined with a sparse crystallization matrix at 4°C and 16°C temperatures using the sitting-drop vapor-diffusion technique with MCSG crystallization suite (Microlytic), Pi-minimal and Pi-PEG screens (Jena Bioscience) (Gorrec *et al.*, 2011). Several conditions yielded diffraction quality crystals. The primary diffracting MdbA crystals were obtained from G9 conditions of Pi-PEG screen (2.9% PEG 350 MME, 34.3% PEG 600, 50 mM Tris buffer pH 7.6) at 16°C after 2 weeks. Due to poor quality and anisotropicity of diffraction, the crystals were used for microseeding using Seed Bead (Hampton Research) against all conditions of Pi-PEG screen at several temperatures. The best MdbA crystals were obtained from F10 conditions of Pi-PEG screen (4.3% PEG 2000, 28.6% PEG 550 MME, 50 mM Tris buffer pH 8.0) at room temperature. The MdbA crystals selected for data collection were washed in Parathone-N oil and flash-cooled in liquid nitrogen.

Single-wavelength X-ray diffraction data were collected at 100 K temperature at the 19-ID beamline of the Structural Biology Center (Rosenbaum *et al.*, 2006) at the Advanced Photon Source at Argonne National Laboratory using the program SBCcollect. The intensities were integrated and scaled with the HKL3000 suite (Minor *et al.*, 2006).

The structure was determined by single-wavelength anomalous dispersion (SAD) phasing using HKL3000 suite (Adams *et al.*, 2002) incorporating SHELXC, SHELXD, SHELXE (Sheldrick, 2010), MLPHARE, SOLVE/RESOLVE (Terwilliger, 2003) programs. Several rounds of manual adjustments of structure models using COOT (Emsley and Cowtan, 2004) and refinements with Refmac program (Murshudov *et al.*, 1997) from CCP4 suite (Collaborative Computational Project, 1994) were done. The stereochemistry of the structure was validated with PHENIX suite (Adams *et al.*, 2002) incorporating MOLPROBITY (Davis *et al.*, 2004) tools. A summary of data collection and refinement statistics is given in Tables 1 and 2. The MdbA atomic coordinates and structure factors were deposited into the Protein Data Bank as 5C00.

Electron microcopy

Bacteria grown on HIA plates or liquid media were suspended and washed in 0.1M NaCl, and then resuspended in PBS. To examine the cells by electron microscopy, 7 μL of culture was placed onto carbon-coated nickel grids (Electron Microscopy Sciences) for 1 min, washed three times with sterile water and then stained with 1% uranyl-acetate for another minute. For immuno-gold labeling, 7 μL of culture was placed onto the grids for 1 min and then washed in PBS 1% BSA three times. The grids were subsequently blocked in PBS 1% BSA with 0.1% gelatin for 1 h at room temperature. Pili were stained with undiluted depleted α-SpaA diluted in PBS 1% BSA for 1 h, and then washed three times in PBS 1% BSA. Grids were blocked again in gelatin for 30 min, washed once and then stained with secondary antibody conjugated to 12 nm gold particles diluted 1:20 in PBS 1% BSA for 1 h. Finally, the samples were washed five times with sterile water and stained with 1% uranyl acetate for 1 min. All samples were viewed using a JEOL JEM-1400 electron microscope.

Van-FL fluorescence microscopy

Overnight cultures of *C. diphtheriae* were diluted 1:50 and then grown at 30°C or 37°C until reaching log phase. A 1:1 mixture of vancomycin (Van) and Van-FL was added to cultures at a concentration of 1 μg ml^{-1}, and incubated for 10 min with agitation at 37°C. The samples were then placed on agar pads and viewed by a fluorescence microscope using excitation/emission wavelengths 504 nm/510 nm.

Spot dilution assays

Spot dilutions of *C. diphtheriae* were performed using overnight cultures grown at 30°C. To test for temperature sensitivity, *C. diphtheriae* cultures were spotted (10^{-3}–10^{-6}) onto HI agar plates, and then incubated at 37°C for 24 h or 30°C for 48 h. To test for antibiotic sensitivity, *C. diphtheriae* were spotted (10^{-3}–10^{-6}) into HI agar plates containing various concentrations of ampicillin or penicillin, and incubated at 30°C for 48 h. The concentrations of antibiotics chosen were based on previous calculations of antimicrobial MICs for *C. diphtheriae* (Soriano *et al.*, 1995).

Alkylation of pilus proteins and diphtheria toxin

C. diphtheriae SpaA monomers were collected from the medium fraction of *C. diphtheriae* HT3, a mutant that secretes monomeric SpaA pilins into the culture medium due to the absence of sortases (Swaminathan *et al.*, 2007). Bacteria were grown to mid-log phase, SpaA were isolated from the medium fraction of mid-log phase grown bacteria by centrifugation, TCA precipitated and acetone washed. To alkylate SpaA, samples were reduced in DTT-containing buffer (100 mM Tris-HCl, 1% SDS, 100 mM DTT, pH 8) at room temperature for 1 h, followed by TCA precipitation and acetone wash to remove the DTT. The resulting pellets were treated with Mal-PEG in alkylation buffer (100 mM Tris-HCl pH 6.8, 1% SDS, 20 mM Mal-PEG) at room temperature for 1 h, followed by TCA precipitation and acetone wash. Protein samples were then dissolved in SDS-loading buffer and separated by 3–20% Tris-glycine gels for immunoblotting with α-SpaA.

To alkylate DT, overnight cultures of *C. diphtheriae* were diluted 1:50 and grown at 30°C until reaching an OD_{600} between 0.2 and 0.3. At this point, 10 $mgmL^{-1}$ of iron chelator ethylenediamine-di-(o-hydroxyphenylacetic) acid (EDDA) was added to the cell cultures to induce DT production for 2 h. DT was isolated from the culture medium by centrifugation, and then TCA precipitated and acetone washed. Alkylation of DT by Mal-PEG was then performed as described in the previous section. DT protein was detected by immunoblotting with a monoclonal antibody generated against the A fragment of DT (Santa Cruz Biotechnology).

Furin cleavage of diphtheria toxin

Similar to the DT alkylation experiment, EDDA was added to liquid cultures of *C. diphtheriae* to induce toxin production. DT was collected from the culture medium by centrifugation, and then concentrated using an Ultracel-30K centrifugal filter (Amicon). Equal volumes of sample were then resuspended in Furin cleavage buffer (100 mM HEPES pH 7.0, 1 mM Cacl2), combined with 2U of Furin convertase (Thermo-Scientific) and incubated at 37°C for 2h. The reactions were then terminated by the addition of SDS loading buffer with or without 2-β-mercaptoethanol, and DT was detected using a monoclonal antibody generated against the A fragment of DT (Santa Cruz Biotechnology).

Infection of guinea pigs

For infection, mid-log phase *C. diphtheriae* cells grown in HI broth at 30°C were collected by centrifugation, washed and resuspended in PBS. Groups of six Hartley guinea pigs (4–5 week-old) were infected via intraperitonal injections with 2.5×10^7 CFUs of each bacterial strain. Animal survival was examined over 7 days, but severely moribund guinea pigs were humanely euthanized. The survival curves were analyzed using Mantel–Cox and chi-square tests.

The procedure above was approved by the Institutional Animal Care and Use Committee (IACUC) for the University of Texas Health Science Center at Houston (UTH). The UTH IACUC adheres to the NIH Office of Laboratory Animal Welfare standards.

Supplementary Material

Refer to Web version on PubMed Central for supplementary material.

Acknowledgments

We thank Timothy Fothergill and Shilpa Muralidhar for technical assistance, members of the Structural Biology Center at Argonne National Laboratory for their help in conducting X-ray diffraction data collection, and our laboratory members for the critical review and discussion of the manuscript. M.E.R.-R. was previously supported by the Predoctoral Training Program in Molecular Basis of Infectious Diseases, National Institute of Allergy and Infectious Diseases (NIH Grant T32 AI55449). This work was supported by the National Institute of General Medical Sciences grant GM094585 (to J.O. and A.J.) and the National Institute of Dental and Craniofacial Research under award numbers F31DE024004 (to M.E.R.-R.) and DE025015 (to H.T.-T.). Argonne is operated by UChicago Argonne, LLC, for the U.S. Department of Energy, Office of Biological and Environmental Research under contract DE-AC02-06CH11357.

References

Adams PD, Grosse-Kunstleve RW, Hung LW, Ioerger TR, McCoy AJ, Moriarty NW, et al. PHENIX: building new software for automated crystallographic structure determination. Acta Crystallogr D Biol Crystallogr. 2002; 58:1948–1954. [PubMed: 12393927]

Bardwell JC, McGovern K, Beckwith J. Identification of a protein required for disulfide bond formation in vivo. Cell. 1991; 67:581–589. [PubMed: 1934062]

Bardwell JC, Lee JO, Jander G, Martin N, Belin D, Beckwith J. A pathway for disulfide bond formation in vivo. Proc Natl Acad Sci USA. 1993; 90:1038–1042. [PubMed: 8430071]

Bayan N, Houssin C, Chami M, Leblon G. Mycomembrane and S-layer: two important structures of *Corynebacterium glutamicum* cell envelope with promising biotechnology applications. J Biotechnol. 2003; 104:55–67. [PubMed: 12948629]

Boquet P, Pappenheimer AM Jr. Interaction of diphtheria toxin with mammalian cell membranes. J Biol Chem. 1976; 251:5770–5778. [PubMed: 965389]

Burkovski A. Cell envelope of corynebacteria: structure and influence on pathogenicity. ISRN Microbiol. 2013; 2013:935736. [PubMed: 23724339]

Chim N, Harmston CA, Guzman DJ, Goulding CW. Structural and biochemical characterization of the essential DsbA-like disulfide bond forming protein from *Mycobacterium tuberculosis*. BMC Struct Biol. 2013; 13:23. [PubMed: 24134223]

Collaborative Computational Project, N. The CCP4 suite: programs for protein crystallography. Acta Crystallogr D Biol Crystallogr. 1994; 50:760–763. [PubMed: 15299374]

Collier RJ. Understanding the mode of action of diphtheria toxin: a perspective on progress during the 20th century. Toxicon. 2001; 39:1793–1803. [PubMed: 11595641]

Crow A, Lewin A, Hecht O, Carlsson Moller M, Moore GR, Hederstedt L, Le Brun NE. Crystal structure and biophysical properties of *Bacillus subtilis* BdbD. An oxidizing thiol:disulfide oxidoreductase containing a novel metal site. J Biol Chem. 2009; 284:23719–23733. [PubMed: 19535335]

Daniels R, Mellroth P, Bernsel A, Neiers F, Normark S, von Heijne G, Henriques-Normark B. Disulfide bond formation and cysteine exclusion in gram-positive bacteria. J Biol Chem. 2010; 285:3300–3309. [PubMed: 19940132]

Davey L, Ng CK, Halperin SA, Lee SF. Functional analysis of paralogous thiol-disulfide oxidoreductases in *Streptococcus gordonii*. J Biol Chem. 2013; 288:16416–16429. [PubMed: 23615907]

Davis IW, Murray LW, Richardson JS, Richardson DC. MOLPROBITY: structure validation and all-atom contact analysis for nucleic acids and their complexes. Nucleic Acids Res. 2004; 32:W615–W619. [PubMed: 15215462]

Dorenbos R, Stein T, Kabel J, Bruand C, Bolhuis A, Bron S, et al. Thiol-disulfide oxidoreductases are essential for the production of the lantibiotic sublancin 168. J Biol Chem. 2002; 277:16682–16688. [PubMed: 11872755]

Dumoulin A, Grauschopf U, Bischoff M, Thony-Meyer L, Berger-Bachi B. *Staphylococcus aureus* DsbA is a membrane-bound lipoprotein with thiol-disulfide oxidoreductase activity. Arch Microbiol. 2005; 184:117–128. [PubMed: 16177891]

Dutton RJ, Boyd D, Berkmen M, Beckwith J. Bacterial species exhibit diversity in their mechanisms and capacity for protein disulfide bond formation. Proc Natl Acad Sci USA. 2008; 105:11933–11938. [PubMed: 18695247]

Emsley P, Cowtan K. Coot: model-building tools for molecular graphics. Acta Crystallogr D Biol Crystallogr. 2004; 60:2126–2132. [PubMed: 15572765]

Gorrec F, Palmer CM, Lebon G, Warne T. Pi sampling: a methodical and flexible approach to initial macromolecular crystallization screening. Acta Crystallogr D Biol Crystallogr. 2011; 67:463–470. [PubMed: 21543849]

Gupta RS. Protein phylogenies and signature sequences: a reappraisal of evolutionary relationships among archaebacteria, eubacteria, and eukaryotes. Microbiol Mol Biol Rev. 1998; 62:1435–1491. [PubMed: 9841678]

Heras B, Kurz M, Jarrott R, Shouldice SR, Frei P, Robin G, et al. *Staphylococcus aureus* DsbA does not have a destabilizing disulfide. A new paradigm for bacterial oxidative folding. J Biol Chem. 2008; 283:4261–4271. [PubMed: 18077463]

Heras B, Shouldice SR, Totsika M, Scanlon MJ, Schembri MA, Martin JL. DSB proteins and bacterial pathogenicity. Nat Rev Microbiol. 2009; 7:215–225. [PubMed: 19198617]

Holm L, Rosenstrom P. Dali server: conservation mapping in 3D. Nucleic Acids Res. 2010; 38:W545–W549. [PubMed: 20457744]

Kadokura H, Beckwith J. Detecting folding intermediates of a protein as it passes through the bacterial translocation channel. Cell. 2009; 138:1164–1173. [PubMed: 19766568]

Kanehisa M, Goto S. KEGG: Kyoto encyclopedia of genes and genomes. Nucleic Acids Res. 2000; 28:27–30. [PubMed: 10592173]

Kang HJ, Paterson NG, Gaspar AH, Ton-That H, Baker EN. The *Corynebacterium diphtheriae* shaft pilin SpaA is built of tandem Ig-like modules with stabilizing isopeptide and disulfide bonds. Proc Natl Acad Sci USA. 2009; 106:16967–16971. [PubMed: 19805181]

Kobayashi T, Ito K. Respiratory chain strongly oxidizes the CXXC motif of DsbB in the *Escherichia coli* disulfide bond formation pathway. EMBO J. 1999; 18:1192–1198. [PubMed: 10064586]

van der Kooi-Pol MM, Reilman E, Sibbald MJ, Veenstra-Kyuchukova YK, Kouwen TR, Buist G, van Dijl JM. Requirement of signal peptidase ComC and thiol-disulfide oxidoreductase DsbA for optimal cell surface display of pseudopilin ComGC in *Staphylococcus aureus*. Appl Environ Microbiol. 2012; 78:7124–7127. [PubMed: 22820325]

Kosuri P, Alegre-Cebollada J, Feng J, Kaplan A, Ingles-Prieto A, Badilla CL, et al. Protein folding drives disulfide formation. Cell. 2012; 151:794–806. [PubMed: 23141538]

London E. Diphtheria toxin: membrane interaction and membrane translocation. Biochim Biophys Acta. 1992; 1113:25–51. [PubMed: 1550860]

Makmura L, Hamann M, Areopagita A, Furuta S, Munoz A, Momand J. Development of a sensitive assay to detect reversibly oxidized protein cysteine sulfhydryl groups. Antioxid Redox Signal. 2001; 3:1105–1118. [PubMed: 11813984]

Mandlik A, Swierczynski A, Das A, Ton-That H. *Corynebacterium diphtheriae* employs specific minor pilins to target human pharyngeal epithelial cells. Mol Microbiol. 2007; 64:111–124. [PubMed: 17376076]

Mandlik A, Swierczynski A, Das A, Ton-That H. Pili in Gram-positive bacteria: assembly, involvement in colonization and biofilm development. Trends Microbiol. 2008; 16:33–40. [PubMed: 18083568]

Martin JL, Bardwell JC, Kuriyan J. Crystal structure of the DsbA protein required for disulphide bond formation in vivo. Nature. 1993; 365:464–468. [PubMed: 8413591]

Meima R, Eschevins C, Fillinger S, Bolhuis A, Hamoen LW, Dorenbos R, et al. The *bdbDC* operon of *Bacillus subtilis* encodes thiol-disulfide oxidoreductases required for competence development. J Biol Chem. 2002; 277:6994–7001. [PubMed: 11744713]

Minor W, Cymborowski M, Otwinowski Z, Chruszcz M. HKL-3000: the integration of data reduction and structure solution – from diffraction images to an initial model in minutes. Acta Crystallogr D Biol Crystallogr. 2006; 62:859–866. [PubMed: 16855301]

Missiakas D, Georgopoulos C, Raina S. Identification and characterization of the *Escherichia coli* gene *dsbB*, whose product is involved in the formation of disulfide bonds in vivo. Proc Natl Acad Sci USA. 1993; 90:7084–7088. [PubMed: 7688471]

Murshudov GN, Vagin AA, Dodson EJ. Refinement of macromolecular structures by the maximum-likelihood method. Acta Crystallogr D Biol Crystallogr. 1997; 53:240–255. [PubMed: 15299926]

Pappenheimer AM Jr, Uhr JW, Yoneda M. Delayed hypersensitivity. I. Induction of hypersensitivity to diphtheria toxin in guinea pigs by infection with *Corynebacterium diphtheriae*. J Exp Med. 1957; 105:1–9. [PubMed: 13385402]

Premkumar L, Heras B, Duprez W, Walden P, Halili M, Kurth F, et al. essential for optimal growth in *Mycobacterium tuberculosis*, is a DsbA-like enzyme that interacts with VKOR-derived peptides and has atypical features of DsbA-like disulfide oxidases. Acta Crystallogr D Biol Crystallogr. 2969c; 69:1981–1994. [PubMed: 24100317]

Reardon, ME.; Ton-That, H. Assembly and function of *Corynebacterium diphtheriae* pili. In: Burkovski, A., editor. Corynebacterium Diphtheriae and Related Toxigenic Species. Netherlands: Springer; 2013. p. 7

Reardon-Robinson ME, Osipiuk J, Chang C, Wu C, Jooya N, Joachimiak A, et al. A disulfide bond-forming machine is linked to the sortase-mediated pilus assembly pathway in the gram-positive bacterium *Actinomyces oris*. J Biol Chem. 2015; 290:21393–21405. [PubMed: 26170452]

Ren G, Stephan D, Xu Z, Zheng Y, Tang D, Harrison RS, et al. Properties of the thioredoxin fold super-family are modulated by a single amino acid residue. J Biol Chem. 2009; 284:10150–10159. [PubMed: 19181668]

Rogers EA, Das A, Ton-That H. Adhesion by pathogenic corynebacteria. Adv Exp Med Biol. 2011; 715:91–103. [PubMed: 21557059]

Rosenbaum G, Alkire RW, Evans G, Rotella FJ, Lazarski K, Zhang RG, et al. The Structural Biology Center 19ID undulator beamline: facility specifications and protein crystallographic results. J Synchrotron Radiat. 2006; 13:30–45. [PubMed: 16371706]

Schäfer A, Tauch A, Jäger W, Kalinowski J, Thierbach G, Pühler A. Small mobilizable multi-purpose cloning vectors derived from the Escherichia coli plasmids pK18 and pK19: selection of defined deletions in the chromosome of Corynebacterium glutamicum. Gene. 1994; 145:69–73. [PubMed: 8045426]

Sheldrick GM. Experimental phasing with SHELXC/D/E: combining chain tracing with density modification. Acta Crystallogr D Biol Crystallogr. 2010; 66:479–485. [PubMed: 20383001]

Shouldice SR, Heras B, Walden PM, Totsika M, Schembri MA, Martin JL. Structure and function of DsbA, a key bacterial oxidative folding catalyst. Antioxid Redox Signal. 2011; 14:1729–1760. [PubMed: 21241169]

Soriano F, Zapardiel J, Nieto E. Antimicrobial susceptibilities of *Corynebacterium* species and other non-spore-forming gram-positive bacilli to 18 antimicrobial agents. Antimicrob Agents Chemother. 1995; 39:208–214. [PubMed: 7695308]

Stols L, Gu M, Diechkman L, Raffer R, Collart FL, Donnelly ML. A new vector for high-throughput ligation independent cloning encoding a tobacco etch virus protease cleavage site. Protein Expr Purif. 2002; 25:8–15. [PubMed: 12071693]

Swaminathan A, Mandlik A, Swierczynski A, Gaspar A, Das A, Ton-That H. Housekeeping sortase facilitates the cell wall anchoring of pilus polymers in *Corynebacterium diphtheriae*. Mol Microbiol. 2007; 66:961–974. [PubMed: 17919283]

Terwilliger TC. SOLVE and RESOLVE: automated structure solution and density modification. Methods Enzymol. 2003; 374:22–37. [PubMed: 14696367]

Ton-That H, Schneewind O. Assembly of pili on the surface of *Corynebacterium diphtheriae*. Mol Microbiol. 2003; 50:1429–1438. [PubMed: 14622427]

Um SH, Kim JS, Lee K, Ha NC. Structure of a DsbF homologue from *Corynebacterium diphtheriae*. Acta Crystallogr F Struct Biol Commun. 2014; 70:1167–1172. [PubMed: 25195886]

Umeda A, Amako K. Growth of the surface of *Corynebacterium diphtheriae*. Microbiol Immunol. 1983; 27:663–671. [PubMed: 6417458]

Valbuena N, Letek M, Ordonez E, Ayala J, Daniel RA, Gil JA, Mateos LM. Characterization of HMW-PBPs from the rod-shaped actinomycete *Corynebacterium glutamicum*: peptidoglycan synthesis in cells lacking actin-like cytoskeletal structures. Mol Microbiol. 2007; 66:643–657. [PubMed: 17877698]

Walsh MA, Dementieva I, Evans G, Sanishvili R, Joachimiak A. Taking MAD to the extreme: ultrafast protein structure determination. Acta Crystallogr D Biol Crystallogr. 1999; 55:1168–1173. [PubMed: 10329779]

Young RM, Mood GM. Effect of penicillin on infection of guinea pigs with *Corynebacterium diphtheriae*. J Bacteriol. 1945; 50:205–212.

Zuber B, Chami M, Houssin C, Dubochet J, Griffiths G, Daffe M. Direct visualization of the outer membrane of mycobacteria and corynebacteria in their native state. J Bacteriol. 2008; 190:5672–5680. [PubMed: 18567661]

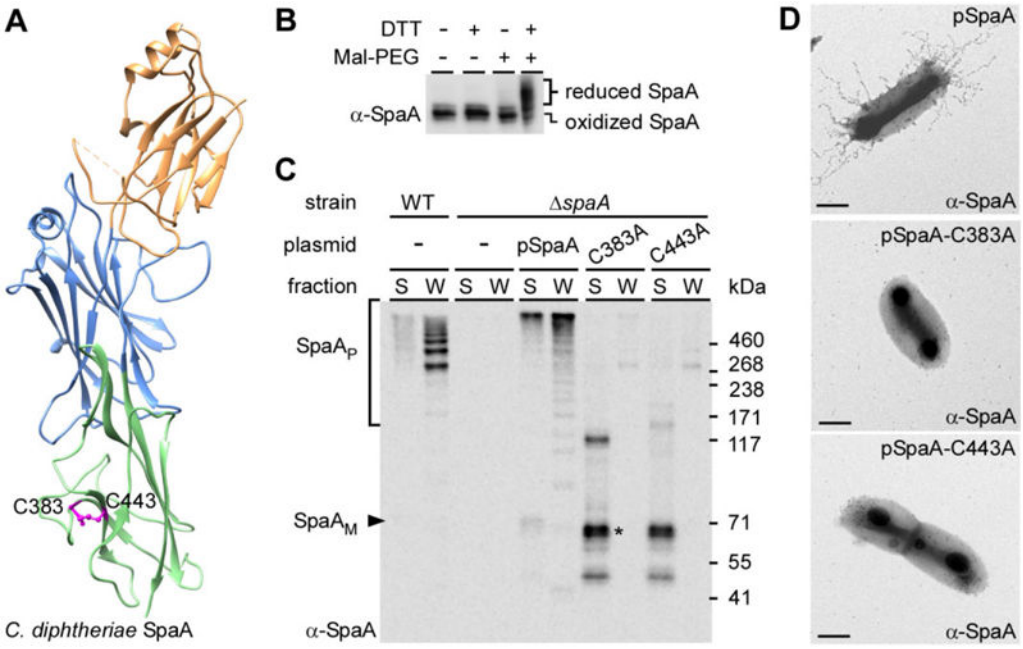

Fig. 1.

Requirement of disulfide bond formation in pilus assembly.

A. Cysteine residues C383 and C443 are predicted to form the C-terminal disulfide bond of the SpaA crystal structure (PDB:3HR6) [25].

B. SpaA monomers were isolated and treated or mock-treated with DTT, followed by Mal-PEG alkylation. The protein samples were immunoblotted with antibodies against SpaA (α-SpaA). Reduced and oxidized forms of SpaA are indicated.

C. Culture medium (S) and cell wall (W) fractions were collected from corynebacterial cultures. Equivalent protein samples obtained by TCA precipitation were immunoblotted with α-SpaA. Monomeric and polymeric forms of SpaA, as well as molecular mass markers (kDa) are indicated. SpaA degraded products are denoted by an asterisk.

D. Cells of corynebacterial strains overexpressing wild-type SpaA (pSpaA) or its isogenic mutants (C383A or C443A) were immobilized on formvar carbon-coated nickel grids, and stained with α-SpaA, followed by anti-rabbit IgG conjugated to gold particles. The samples were then stained with 1% uranyl acetate and viewed by a transmission electron microscope. Scale bars indicate 0.2 μm.

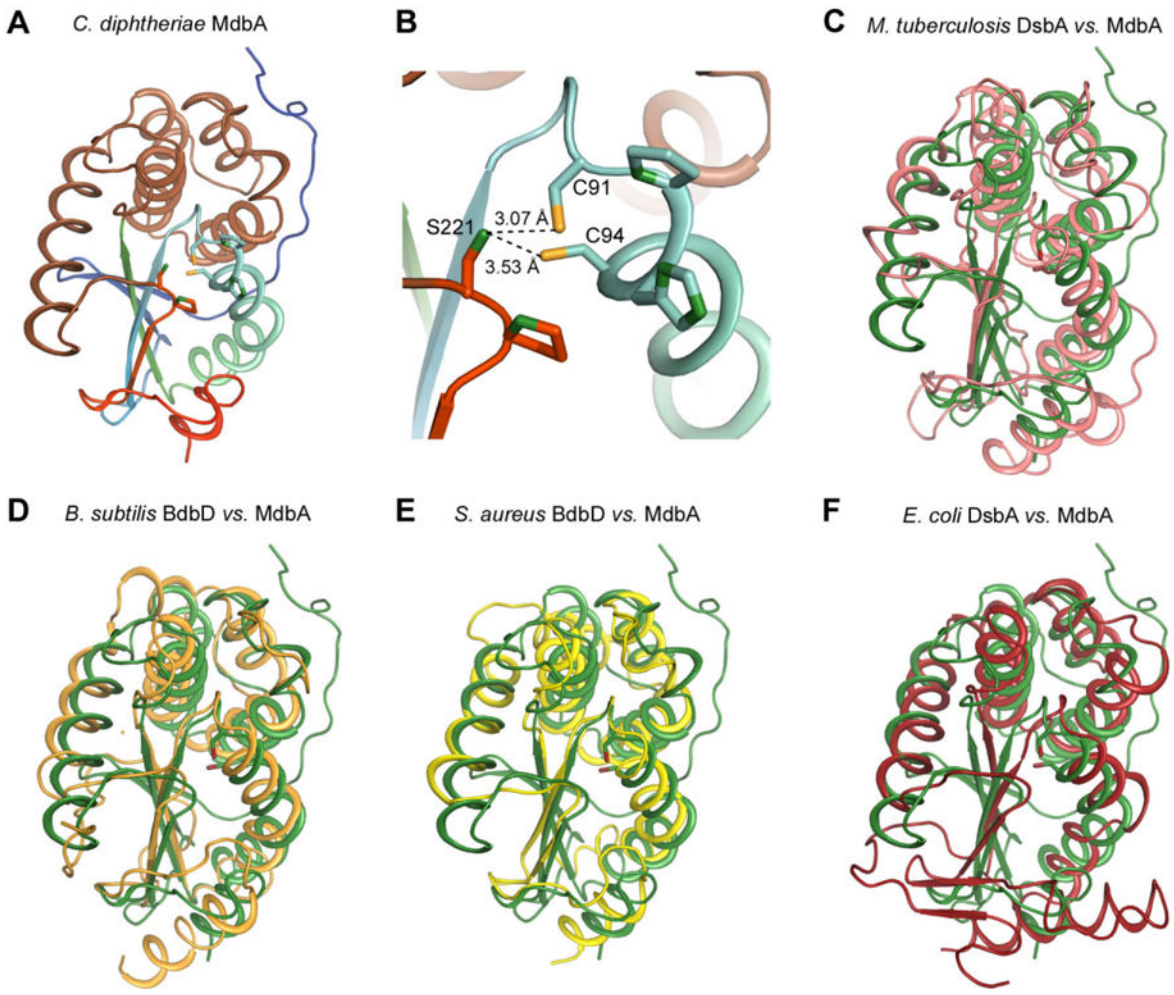

Fig. 2.

Structural analysis of the *C. diphtheriae* disulfide bond-forming protein MdbA.

A. The *C. diphtheriae* MdbA crystal structure (residues 43–244), solved to a 1.77-Å resolution, possesses a thioredoxin-like domain (rainbow colors) and an alpha-helical domain (light brown).

B. The MdbA active site is comprised of C91, P92, H93 and C94. The Sγ group in the two cysteine residues forms a hydrogen bond with S221 of the *Cis*-Pro element.

C–F. The MdbA structure (green) was aligned with *M. tuberculosis* DsbA (C; PDB: 4K6X), *B. subtilis* BdbB (D; PDB:3EU3), *S. aureus* DsbA (E; PDB:3BCI) and *E. coli* DsbA (F; PDB:1A2L).

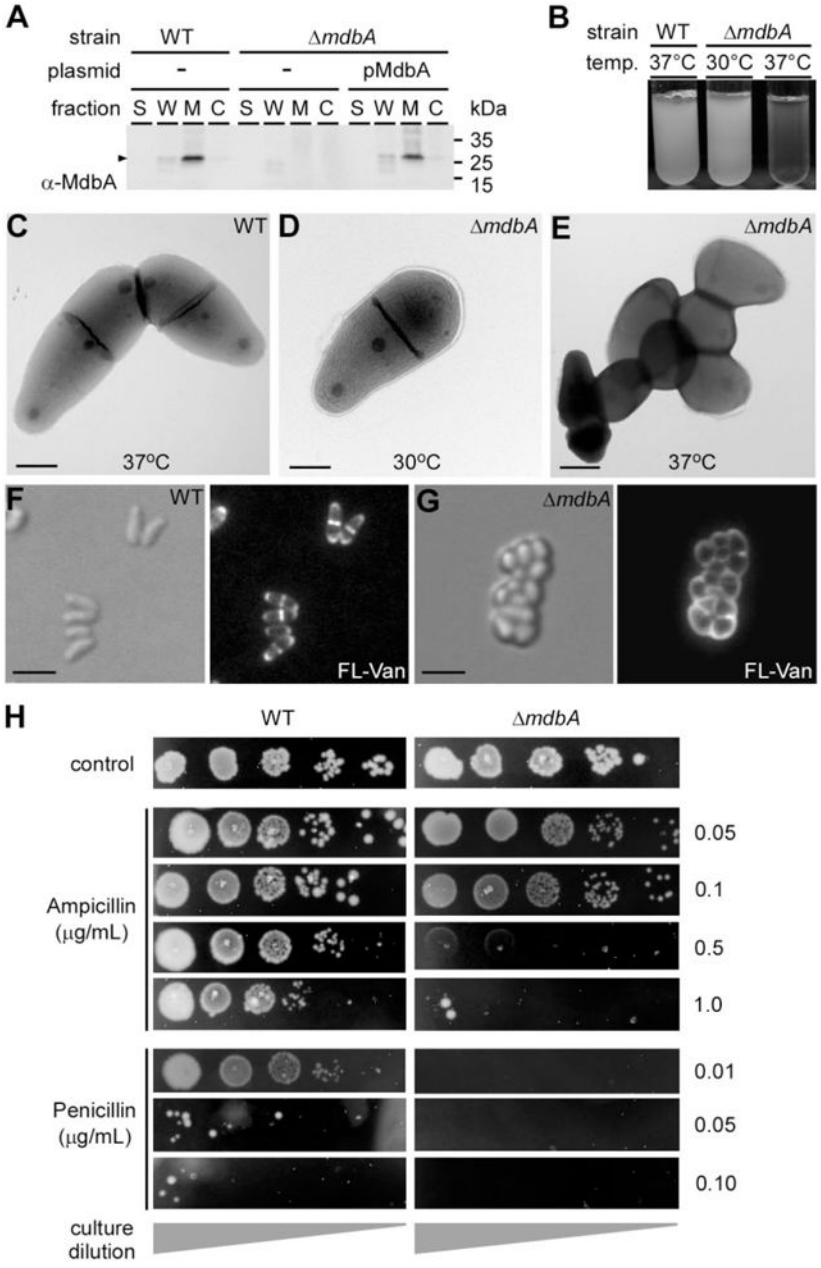

Fig. 3.

The *C. diphtheriae* Δ*mdbA* mutant is defective in cell growth and division.

A. Culture medium (S), cell wall (W), membrane (M) and cytoplasmic (C) fractions were collected from corynebacterial cultures. Protein samples were immunoblotted with antibodies against MdbA (α-MdbA).

B. Single colonies of the *C. diphtheriae* wild-type and *mdbA* mutant strains were inoculated in broth cultures overnight at 37°C or 30°C.

C–E. Stationary cultures of *C. diphtheriae* grown at 30°C were diluted in fresh media, and then incubated at 30°C or 37°C for 5 h. Harvested cells were immobilized on nickel grids,

stained with 1% uranyl acetate and viewed by a transmission electron microscope. Scale bars indicate 0.5 μm.

F–G. Overnight cultures of *C. diphtheriae* grown at 30°C were diluted into fresh media, and then incubated at 37°C until wild-type cells reached log phase. A 1:1 mixture of vancomycin and fluorescent vancomycin (Van-FL) was added to cultures, and incubated for 10 min. The cells were placed directly on agar pads, and viewed by a fluorescence microscope. Scale bars indicate 2.5 μm.

H. Overnight cultures of *C. diphtheriae* grown at 30°C were diluted (10^{-3}–10^{-7}) and spotted on HIA plates containing various concentrations of ampicillin or penicillin, and incubated at 30°C for 48 h.

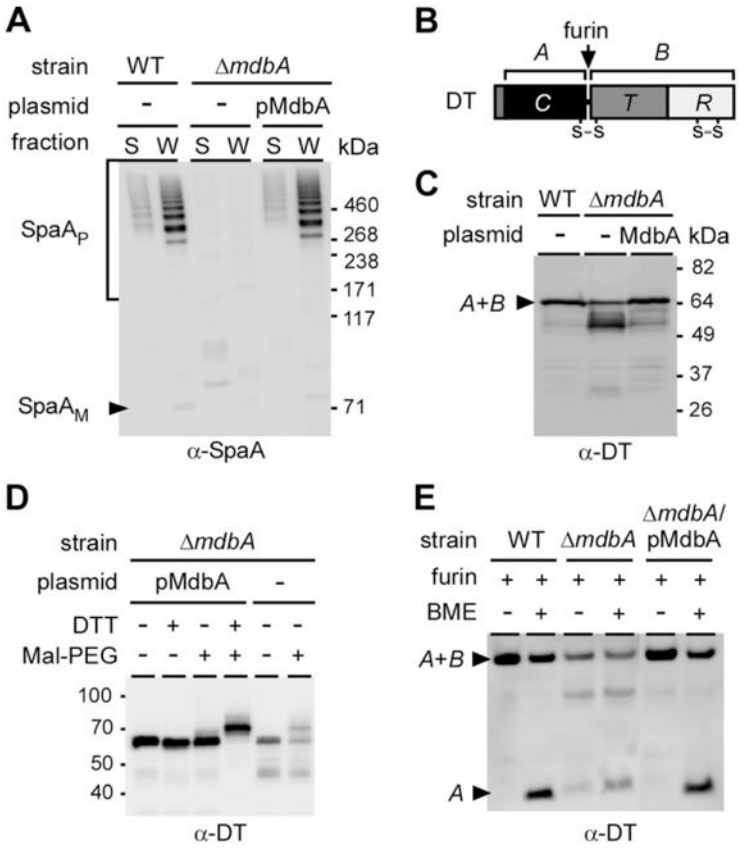

Fig. 4.

Requirement of the disulfide bond-forming machine MdbA for pilus assembly and diphtheria toxin (DT) production in *C. diphtheriae*.

A. Protein samples obtained from *C. diphtheriae* S and W fractions were separated on a 3–12% gradient gel and immunoblotted with α-SpaA.

B. A graphic presentation of DT highlights its two disulfide bonds, with the first one encircling domains A and B. A second disulfide bond is located at the B domain.

C. DT production was induced by addition of the iron chelator EDDA to culture media. Secreted DT was separated from cells by centrifugation and the protein samples were analyzed by Western blotting with monoclonal antibodies against domain A (α-DT).

D. DT collected from the culture medium of *C. diphtheriae* strains expressing or lacking MdbA was treated or mock-treated with DTT, followed by Mal-PEG alkylation. The protein samples were analyzed by immunoblotting with α-DT.

E. DT was collected from culture media, and concentrated by filter centrifugation. The protein was then treated with furin for 2 h at 37°C, boiled in SDS with or without β-mercaptoethanol, separated with a 12% Tris-Glycine gel and immunoblotted with α-DT. DT A and B fragments are indicated. Molecular mass markers are shown.

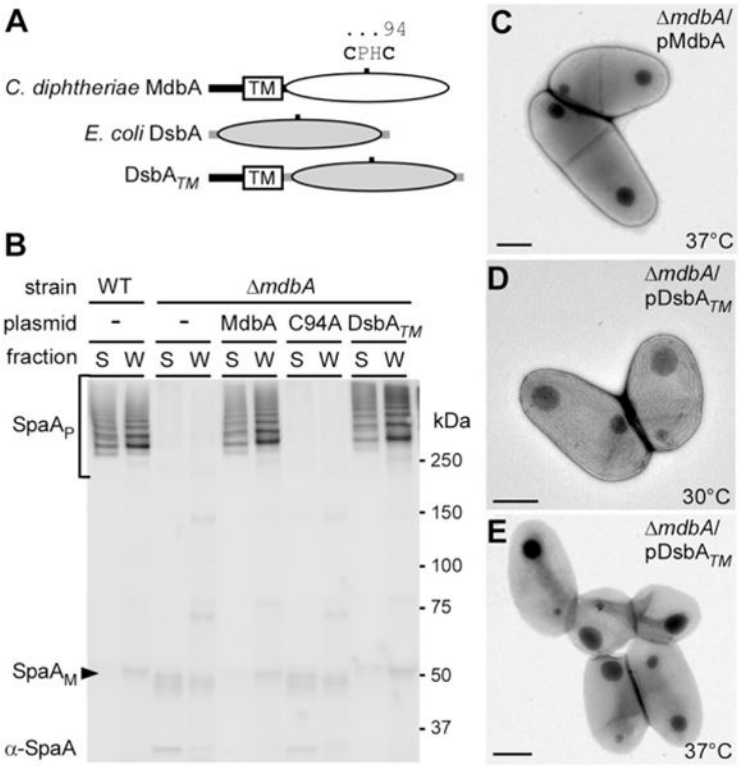

Fig. 5.

Conservation of disulfide bond-forming machinery.

A. A graphical representation of the primary sequences of *C. diphtheriae* MdbA and *E. coli* DsbA. The catalytic CPHC of MdbA is highlighted. To express *E. coli* DsbA in *C. diphtheriae*, the N-terminal signal peptide was swapped with the signal peptide and transmembrane anchor of MdbA.

B. Protein samples obtained from *C. diphtheriae* S and W fractions were separated on a 3–12% gradient gel and immunoblotted with α-SpaA.

C–E. Stationary cultures of *C. diphtheriae* grown at 30°C were diluted in fresh media, and then incubated at 30°C or 37°C for 5 h. Harvested cells were immobilized on nickel grids, stained with 1% uranyl acetate and viewed by a transmission electron microscope. Scale bars indicate 0.5 μm.

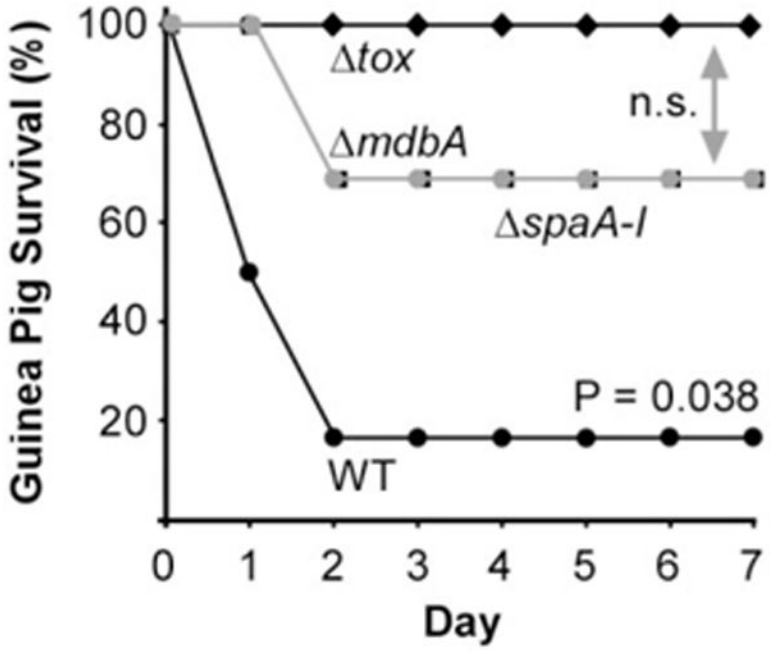

Fig. 6.

Requirement of MdbA for bacterial virulence. Six 4-week-old guinea pigs were infected via IP with ~ 2.5×10^7 corynebacteria of the wild-type (filled circles), pilus-less mutant (filled squares), toxin-less mutant (filled diamonds) or Δ*mdbA* mutant (gray circles) strain. Animal survival was monitored for 7 days. Statistical significance was analyzed by a paired *t*-test using GraphPad; n.s. denotes not significant.

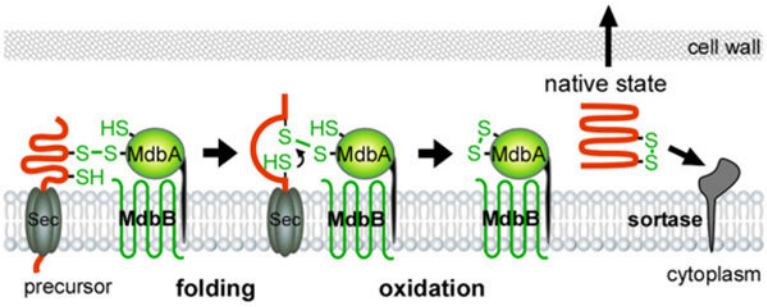

Fig. 7.

A model of MdbA-mediated posttranslocational protein folding. The transmembrane thiol-disulfide oxidoreductase MbdA enzyme forms a mixed disulfide bond with nascent precursors emerging from the Sec translocon, allowing the precursors to fold into a near-native state before MdbA-driven catalysis of disulfide bond formation, resulting in fully folded proteins for subsequent steps. An unidentified membrane-bound oxidoreductase termed MdbB is proposed to reoxidize MdbA.

Table 1

Crystal data collection statistics.

X-ray wavelength (Å)	0.9792	
Space group	P 2_1	
Unit cell dimensions	a = 61.5 Å, b = 76.6 Å, c = 72.6 Å, α = γ = 90°, β = 90.2°	
Resolution[a] (Å)	33.9 – 1.77	(1.80 – 1.77)
No. of unique reflections	65737	(3243)
Completeness (%)	99.9	(99.4)
R-merge	0.078	(0.62)
CC1/2 ($Å^2$)	–	(0.75)
I/σ	9.1	(2.02)
Redundancy	4.8	(4.0)
Molecules per asymmetric unit	4	
No. of protein residues	832	

[a]Numbers in parenthesis are shown for the highest resolution shell.

Table 2

Structure refinement statistics.

Resolution range (Å)	34.0 – 1.77	(1.82 – 1.77)
Reflections	65 716	(4 775)
σ cutoff	None	
R-value (all) (%)	16.42	
R-value (*R*-work) (%)	16.19	(26.9)
Free *R*-value (%)	20.98	(28.1)
Rms deviations from ideal geometry		
Bond length (Å)	0.013	
Angle (degrees)	1.50	
Chiral (Å)	0.093	
No. of atoms		
Protein	6 357	
Water	399	
Mean B-factor (Å^2)		
All atoms	33.6	
Protein atoms	33.5	
Protein main chain	31.7	
Protein side chain	35.2	
Water	33.8	
Molprobity Ramachandran plot statistics		
Residues in favored regions (%)	97.6	
Residues in allowed regions (%)	99.8	
Residues in disallowed region (%)	0.2	